Phytochemistry 72 (2011) 651–661

Contents lists available at ScienceDirect

Phytochemistry

journal homepage: www.elsevier.com/locate/phytochem

Steroidal glycosides from *Ruscus ponticus*

Assunta Napolitano [a], Tamar Muzashvili [b], Angela Perrone [a], Cosimo Pizza [a], Ether Kemertelidze [b], Sonia Piacente [a,*]

[a] Dipartimento di Scienze Farmaceutiche e Biomediche, Università degli Studi di Salerno, Via Ponte Don Melillo, I-84084 Fisciano, Italy
[b] Institute of Pharmacochemistry, P. Sarajishvili Street 36, 0159 Tbilisi, Georgia

ARTICLE INFO

Article history:
Received 23 November 2010
Received in revised form 21 January 2011
Available online 26 February 2011

Keywords:
Ruscus ponticus
Steroidal glycosides
HPLC–ESIMS comparative profile

ABSTRACT

A comparative metabolite profiling of the underground parts and leaves of *Ruscus ponticus* was obtained by an HPLC–ESIMS^n method, based on high-performance liquid chromatography coupled to electrospray positive ionization multistage ion trap mass spectrometry. The careful study of HPLC–ESIMS^n fragmentation pattern of each chromatographic peak, in particular the identification of diagnostic product ions, allowed us to get a rapid screening of saponins belonging to different classes, such as dehydrated/or not furostanol, spirostanol and pregnane glycosides, and to promptly highlight similarities and differences between the two plant parts. This approach, followed by isolation and structure elucidation by 1D- and 2D-NMR experiments, led to the identification of eleven saponins from the underground parts, of which two dehydrated furostanol glycosides and one vespertilin derivative, and nine saponins from *R. ponticus* leaves, never reported previously. The achieved results highlighted a clean prevalence of furostanol glycoside derivatives in *R. ponticus* leaves rather in the underground parts of the plant, which showed a wider structure variety. In particular, the occurrence of dehydrated furostanol derivatives, for the first time isolated from a *Ruscus* species, is an unusual finding which makes unique the saponins profile of *R. ponticus*.

1. Introduction

Ruscus ponticus Woronow ex grossh. (Ruscaceae) is an evergreen, perennial, 30–50 cm tall shrub-like relict plant, with folium-like cladodes and red fruits, widespread in Crimea and Caucasus, particularly in the forests of West and East Georgia (Gagnidze, 2005). *R. ponticus* is well known in this country for the preparation of ruscoponin, obtained from the underground parts of the plant. Some pharmacological properties of ruscoponin, containing steroidal glycosides, were studied. In particular, it causes lysis of fibrin in *vitro* (Kereselidze et al., 1975) and exhibits a pronounced antiexudative effect, proving to be a low-toxic (LD_{50} 3.17 g/kg) phlebodynamic and antiexudative remedy (Mulkijanyan and Abuladze, 1998, 2000). It is effective when administered either systemically or locally, and does not reveal undesirable side effects (Mulkijanyan and Abuladze, 1998, 2000).

Notwithstanding this, few phytochemical studies on *R. ponticus* are reported in literature: so far only diosgenin and neoruscogenin were found in the roots of *R. ponticus* (Pkheidze et al., 1971), along with steroidal glycosides namely ruscoponticosides C, D, and E (Korkashvili et al., 1985). Furthermore, there is only one report about the steroidal composition of the leaves of *R. ponticus* (Pkheidze et al., 1970).

Recently, we have developed an analytical method, based on high-performance liquid chromatography coupled to electrospray positive ionization multistage ion trap mass spectrometry (HPLC–ESIMS^n), as an effective tool to rapidly identify and guide the isolation of target saponins from the leaves of *Ruscus colchicus* Y. Yeo (Perrone et al., 2009).

This HPLC–ESIMS^n method allowed to define the mass fragmentation pathways of different types of steroidal glycosides, and to screen saponins belonging to different classes. Thus it can be used to obtain rapid information about saponin composition of different plants or parts of the same plant, allowing a rapid comparative metabolite profiling of target matrixes.

Thereby, in order to fill the gap about *R. ponticus* composition, we decided to carry out the phytochemical analysis of both the underground parts and leaves of *R. ponticus*, with the double aim to determine their main constituents and to ascertain the differences in their steroidal composition. In this way, 11 compounds from *R. ponticus* underground parts, 3 of which new (**5**, **7**–**8**), and 9 compounds from *R. ponticus* leaves, all found to be new compounds (**12**–**20**), were identified.

2. Results and discussion

To obtain a rapid comparative steroidal profiling of the underground parts and leaves of *R. ponticus*, positive HPLC–ESIMS^n profiles of the ethanol extracts of both parts were obtained by using

* Corresponding author. Tel.: +39 089969763; fax: +39 089969602.
E-mail address: piacente@unisa.it (S. Piacente).

0031-9422/$ - see front matter © 2011 Elsevier Ltd. All rights reserved.
doi:10.1016/j.phytochem.2011.01.033

the same analytical conditions (Fig. 1). Under these conditions, 11 chromatographic peaks (**1**–**11**) in the HPLC–ESIMS^n profile of underground parts and 9 chromatographic peaks (**12**–**20**) in the HPLC–ESIMS^n profile of leaves were displayed. A careful analysis of ESIMS^n spectra recorded for each chromatographic peak allowed us to preliminarily define the presence of at least two classes of compounds, yielding the first abundant $[(M-ROH)+H]^+$ ions and the second main $[M+H]^+$ and $[M+Na]^+$ ions (Table 1). This behavior permitted us a first metabolite screening between furostanol glycosides, possessing a labile hydroxy or methoxy group at C-22 and thereby responsible for the formation of intense $[(M-ROH)+H]^+$ ions (**1**–**4**, **12**–**18**) (Perrone et al., 2009), and steroidal glycosides lacking in their structure of this labile group (**5**–**11**, **19**–**20**). According to this analysis, the chromatographic profile of each ethanol extract showed a clean metabolite separation, with the furostanol glycosides eluting before the other steroidal glycosides, and being much more present in the leaves extract than in the underground parts. Analogously to what observed for *R. colchicus*, when furostanol glycosides went along with their relative 22-methyl ethers, in both chromatograms pairs of peaks having the same *m/z* value but different retention times were displayed (**12**, **13** and **15**, **16**) (Table 1) (Perrone et al., 2009). The analysis of the HPLC–ESIMS^n spectra of each chromatographic peak allowed to add a piece in the complex puzzle of *R. ponticus* steroidal composition. In fact, information about the number and the nature (hexose/pentose) of sugar units as well as the aglycon moiety could be obtained by the analysis of full and multistage HPLC–ESIMS^n spectra of each chromatographic peak, observing the subsequent losses of the sugar units from $[(M-ROH)+H]^+$ or $[M+H]^+$ and $[M+Na]^+$ ions until to the aglycon ion peak (Table 1). In this regard, it is noteworthy that most compounds displayed, in HPLC–ESIMS^2 as well as in HPLC–ESIMS^3, a diagnostic neutral loss of 144 or 142 a.m.u., from the $[(M-162)+H]^+$/$[(M-162)+Na]^+$ ions and from the $[(M-ROH-162)+H]^+$ ions (Table 1). This neutral loss could be explained supposing the formation of the 7-hydroxy-6-methylheptan-3-one or the 6-hydroxymethyl-hept-6-en-3-one moiety, respectively, by the opening of the substituted E ring present in spirostanol and dehydrated/or not furostanol glycosides. This result led us to promptly ascertain the presence or not of an exomethylene group on the aglycon moiety, and to easily distinguish spirostanol and dehydrated/or not furostanol glycosides from the other steroidal glycosides. Thereby, it could be preliminarily concluded that, while *R. ponticus* leaves was entirely characterized by dehydrated/or not furostanol saponins, the underground parts of the plant contained also spirostanol glycosides and two compounds (**8** and **9**) belonging to classes of steroidal glycosides differing from these latter. Moreover, the comparative analysis of the full HPLC–ESIMS spectra of the chromatographic peaks due to spirostanol and/or dehydrated furostanol glycosides interestingly highlighted for one pair of compounds (**7**, **20**) the same peculiarity showed by furostanol glycosides, namely the same *m/z* value but different retention times (Table 1). The analysis of HPLC–ESIMS^n spectra of this pair of peaks easily allowed to ascertain for them a different glycosidation pattern and, thereby, a different aglycon moiety. Finally, considering the results inferred from the HPLC–ESIMS^n data of underground parts and leaves of *R. ponticus*

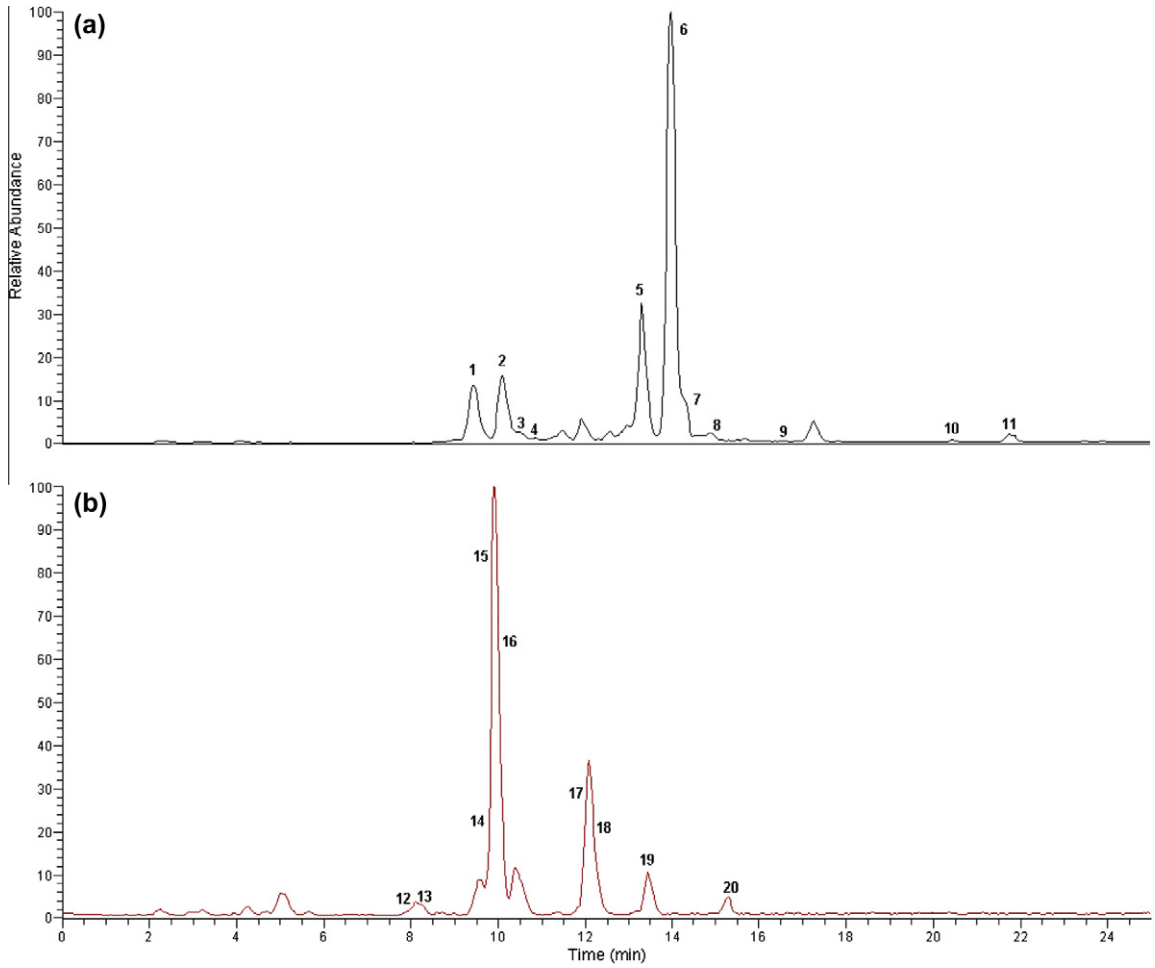

Fig. 1. (a) HPLC–ESIMS profile of the ethanol extract of *R. ponticus* underground parts and (b) HPLC–ESIMS profile of the ethanol extract of *R. ponticus* leaves.

Table 1
ESIMS and ESIMS^n product ions of compounds **5**, **7**, **8**, **12**–**20** isolated from the underground parts and leaves of *R. ponticus*.

Compounds	MW	MS^1	MS^n fragment ions
5	1030	1053 $[M+Na]^+$	891 $[(M-162)+Na]^+$, 749 $[(M-162-142)+Na]^+$, 745 $[(M-162-146)+Na]^+$, 729 $[(M-162-162)+Na]^+$, 613 $[(M-162-146-132)+Na]^+$, 583 $[(M-162-162-146)+Na]^+$, 451 $[(M-162-146-132-162)+Na]^+$
7	870	893 $[M+Na]^+$	747 $[(M-146)+Na]^+$, 731 $[(M-162)+Na]^+$, 615 $[(M-146-132)+Na]^+$, 587 $[(M-162-144)+Na]^+$, 453 $[(M-146-132-162)+Na]^+$, 441 $[(M-162-144-146)+Na]^+$, 309 $[(M-146-132-162-144)+Na]^+$
8	638	661 $[M+Na]^+$	617 $[(M-44)+Na]^+$, 515 $[(M-146)+Na]^+$, 383 $[(M-146-132)+Na]^+$
12	918	901 $[(M-H_2O)+H]^+$ 941 $[M+Na]^+$	739 $[(M-H_2O)-162)+H]^+$, 595 $[(M-H_2O)-162-144)+H]^+$, 593 $[(M-H_2O)-162-146)+H]^+$, 449 $[(M-H_2O)-162-144-146)+H]^+$, 431 $[(M-H_2O)-162-146-162)+H]^+$, 287 $[(M-H_2O)-162-144-146-162)+H]^+$
13	932	901 $[(M-CH_3OH)+H]^+$ 955 $[M+Na]^+$	739 $[(M-CH_3OH)-162)+H]^+$, 595 $[(M-CH_3OH)-162-144)+H]^+$, 593 $[(M-CH_3OH)-162-146)+H]^+$, 449 $[(M-CH_3OH)-162-144-146)+H]^+$, 431 $[(M-CH_3OH)-162-146-162)+H]^+$, 287 $[(M-CH_3OH)-162-144-146-162)+H]^+$
14	958	941 $[(M-H_2O)+H]^+$ 981 $[M+Na]^+$	795 $[(M-H_2O)-146)+H]^+$, 779 $[(M-H_2O)-162)+H]^+$, 735 $[(M-H_2O)-146-60)+H]^+$, 637 $[(M-H_2O)-162-142)+H]^+$, 633 $[(M-H_2O)-162-146)+H]^+$, 573 $[(M-H_2O)-146-60-162)+H]^+$, 491 $[(M-H_2O)-162-142-146)+H]^+$, 431 $[(M-H_2O)-162-142-146-60)+H]^+$, 411 $[(M-H_2O)-146-60-162-162)+H]^+$
15	960	943 $[(M-H_2O)+H]^+$ 983 $[M+Na]^+$	797 $[(M-H_2O)-146)+H]^+$, 781 $[(M-H_2O)-162)+H]^+$, 737 $[(M-H_2O)-146-60)+H]^+$, 637 $[(M-H_2O)-162-144)+H]^+$, 635 $[(M-H_2O)-162-146)+H]^+$, 575 $[(M-H_2O)-162-146-60)+H]^+$, 491 $[(M-H_2O)-162-144-146)+H]^+$, 431 $[(M-H_2O)-162-144-146-60)+H]^+$, 413 $[(M-H_2O)-162-146-60-162)+H]^+$, 269 $[(M-H_2O)-162-144-146-60-162)+H]^+$
16	974	943 $[(M-CH_3OH)+H]^+$ 997 $[M+Na]^+$	797 $[(M-CH_3OH)-146)+H]^+$, 781 $[(M-CH_3OH)-162)+H]^+$, 737 $[(M-CH_3OH)-146-60)+H]^+$, 637 $[(M-CH_3OH)-162-144)+H]^+$, 635 $[(M-CH_3OH)-162-146)+H]^+$, 575 $[(M-CH_3OH)-162-146-60)+H]^+$, 491 $[(M-CH_3OH)-162-144-146)+H]^+$, 431 $[(M-CH_3OH)-162-144-146-60)+H]^+$, 413 $[(M-CH_3OH)-162-146-60-162)+H]^+$, 269 $[(M-CH_3OH)-162-144-146-60-162)+H]^+$
17	886	869 $[(M-H_2O)+H]^+$ 909 $[M+Na]^+$	737 $[(M-H_2O)-132)+H]^+$, 707 $[(M-H_2O)-162)+H]^+$, 575 $[(M-H_2O)-162-132)+H]^+$, 565 $[(M-H_2O)-162-142)+H]^+$, 433 $[(M-H_2O)-162-142-132)+H]^+$, 413 $[(M-H_2O)-162-132-162)+H]^+$, 271 $[(M-H_2O)-162-142-132-162)+H]^+$
18	888	871 $[(M-H_2O)+H]^+$ 911 $[M+Na]^+$	739 $[(M-H_2O)-132)+H]^+$, 709 $[(M-H_2O)-162)+H]^+$, 577 $[(M-H_2O)-162-132)+H]^+$, 565 $[(M-H_2O)-162-144)+H]^+$, 433 $[(M-H_2O)-162-144-132)+H]^+$, 415 $[(M-H_2O)-162-132-162)+H]^+$, 271 $[(M-H_2O)-162-144-132-162)+H]^+$
19	942	943 $[M+H]^+$	797 $[(M-146)+H]^+$, 781 $[(M-162)+H]^+$, 737 $[(M-146-60)+H]^+$, 637 $[(M-162-144)+H]^+$, 635 $[(M-162-146)+H]^+$, 575 $[(M-162-146-60)+H]^+$, 491 $[(M-162-144-146)+H]^+$, 431 $[(M-162-144-146-60)+H]^+$, 413 $[(M-162-146-60-162)+H]^+$, 269 $[(M-162-144-146-60-162)+H]^+$
20	870	871 $[M+H]^+$	739 $[(M-132)+H]^+$, 709 $[(M-162)+H]^+$, 577 $[(M-162-132)+H]^+$, 565 $[(M-162-144)+H]^+$, 433 $[(M-162-144-132)+H]^+$, 415 $[(M-162-132-162)+H]^+$, 271 $[(M-162-144-132-162)+H]^+$

(Table 1), and comparing them with those obtained from the HPLC–ESIMS^n analysis of *R. colchicus* leaves (Perrone et al., 2009), we could to claim that among all the 20 compounds detected in both *R. ponticus* extracts only one, ruscoponticoside E (**2**), was already present in *R. colchicus* leaves.

At this point, to unambiguously elucidate these unknown metabolites by NMR experiments, in particular ascertaining for compounds **5**–**7**, **10**–**11**, and **19**–**20** the spirostanol or dehydrated furostanol identity, all compounds from the underground parts and leaves of *R. ponticus* were isolated and purified.

The analysis of positive HRMALDITOFMS spectrum of each compound allowed to unambiguously assign them the respective molecular formula. To determine the absolute configuration of the sugar units, the crude saponin mixture has been submitted to acid hydrolysis yielding D-glucose, L-rhamnose and L-arabinose; the absolute configurations of the sugar units were established by comparison of their optical rotation values with those reported in the literature (Belitz et al., 2009; Wang et al., 2008).

By comparison of the spectroscopic data with literature values, eight known compounds (**1**–**4**, **6**, **9**–**11**) were identified in *R. ponticus* undergrounds, in particular five furostanol derivatives namely 26-*O*-β-D-glucopyranosyl-furosta-5,25(27)-diene-1β,3β,22α,26-tetrol 1-*O*-[β-D-glucopyranosyl-(1→3)-*O*-α-L-rhamnopyranosyl-(1→ 2)-*O*-α-L-arabinopyranoside] (ruscoside) (**1**) (Bombardelli et al., 1972), 26-*O*-β-D-glucopyranosyl-furosta-5,25(27)-diene-1β,3β,22α ,26-tetrol 1-*O*-α-L-rhamnopyranosyl-(1→2)-*O*-α-L-arabinopyranoside (ruscoponticoside E) (**2**) (Bombardelli et al., 1972; Korkashvili et al., 1985), 26-*O*-β-D-glucopyranosyl-22α-methoxy-furosta-5,25(27)-diene-1β,3β,26-triol 1-*O*-α-L-rhamnopyranosyl-(1→2) -*O*-α-L-arabinopyranoside (**3**) (Mimaki et al., 1998), (25*R*)-26-*O*-β-D-glucopyranosyl-22α-methoxy-furost-5-ene-1β,3β,26-triol 1-*O*-α-L-rhamnopyranosyl-(1→2)-*O*-α-L-arabinopyranoside (ceparoside A) (**4**) (Yuan et al., 2008), 26-*O*-β-D-glucopyranosyl-furosta-5,20(22),25(27)-triene-1β,3β,26-triol 1-*O*-[α-L-rhamnopyranosyl-(1→2)-O-α-L-arabinopyranoside] (**6**) (Mimaki et al., 1996), the pregnane derivative namely 1β,3β-dihydroxypregna-5,16-dien-20-one 1-*O*-α-L-rhamnopyranosyl-(1→2)-*O*-α-L-arabinopyranoside (**9**) (Bombardelli et al., 1972), along with two spirostanol derivatives namely spirosta-5,25(27)-diene-1β,3β-diol 1-*O*-[β-D-glucopyranosyl-(1→3)-*O*-α-L-rhamnopyranosyl-(1→2)-*O*-α-L-arabinopyranoside] (ruscoponticoside D) (**10**) (Korkashvili et al., 1985) and spirosta-5,25(27)-diene-1β,3β-diol 1-*O*-α-L-rhamnopyranosyl-(1→2)-*O*-α-L-arabinopyranoside (ruscoponticoside C) (**11**) (Korkashvili et al., 1985).

According to the HPLC–ESIMS^n results, the full positive ESIMS spectrum of compound **5** was consistent with a not furostanolic saponin, showing in fact as main peak the $[M+Na]^+$ ion at *m/z* 1053 (Table 1). The analysis of the ESIMS^n spectra of **5** allowed to confirm this result and to ascertain the spirostanol or dehydrated furostanol nature of this compound, showing a characteristic product ion at *m/z* 749, originating from the $[(M-162)+Na]^+$ peak ion by neutral loss of the 6-hydroxymethyl-hept-6-en-3-one moiety (142 a.m.u.). Moreover, the ESIMS^2 spectrum of the ion at *m/z* 1053 showed a fragmentation pattern in agreement with the presence of one hexose, one deoxy-hexose, and one pentose moieties, as described in Table 1. The ^{1}H NMR spectrum of **5** showed signals for three tertiary methyl groups at δ 1.63 (3H, *s*), 1.13 (3H, *s*) and 0.75 (3H, *s*), exomethylene protons at δ 5.93 and 4.96 (each 1H, *br s*), an olefinic proton at δ 5.59 (1H, *br d*, J = 5.7 Hz), three methine proton signals at δ 4.74 (1H, *dt*, J = 10.1, 7.8, 5.3 Hz), 3.40 (1H, *dd*, J = 11.9, 3.9 Hz) and 3.38 (1H, *m*), indicative of secondary alcoholic functions, two methylene proton signals at δ 4.36 and 4.15 (each 1H, *d*, J = 12.1 Hz), ascribable to a primary alcoholic function, along with four anomeric protons at δ 5.33 (1H, *d*, J = 1.2 Hz), 4.57 (1H, *d*, J = 7.5 Hz), 4.31 (1H, *d*, J = 7.5 Hz) and 4.30 (1H, *d*, J = 3.7 Hz) and a secondary methyl group at δ 1.29 (3H, *d*, J = 6.0 Hz). The ^{13}C NMR spectrum displayed for the aglycon signals ascribable to six sp^2 carbons at δ 152.1,

105.4, 146.4, 139.5, 125.7 and 112.7, three secondary alcoholic functions at δ 85.7, 84.3 and 68.8, and one primary alcoholic function at δ 72.1, suggesting the occurrence of a furostanol skeleton with a $\Delta^{20,22}$ double bond (Mimaki et al., 1996). The occurrence of a $\Delta^{20,22}$ double bond was confirmed from the HMBC spectrum which showed significative cross-peaks between the proton signal of Me-21 (δ 1.63) and C-20 (δ 105.4)/C-22 (δ 152.1). On the basis of the HSQC and HMBC correlations, the aglycon moiety of compound **5** was identified as furosta-5,20(22),25(27)-triene-1β,3β,26-triol (Table 2). It was evident from the ^{1}H and ^{13}C NMR data that the sugar chain of **5** consisted of four sugar units. The chemical shifts of all the individual protons of the four sugar units were ascertained from a combination of 1D-TOCSY and DQF-COSY spectral analysis, and the ^{13}C chemical shifts of their relative attached carbons were assigned unambiguously from the HSQC spectrum (Table 5). These data showed the presence of two β-glucopyranosyl units (δ 4.57 and 4.31), one α-arabinopyranosyl (δ 4.30) and one α-rhamnopyranosyl unit (δ 5.33). The α configuration of the rhamnopyranosyl unit was deduced from the value of J_{H1-H2} coupling (J = 1.2 Hz) and from the absence of intraresidual ROESY correlations between H-1$_{rha}$ and H-3$_{rha}$/H-5$_{rha}$. It was also confirmed by the H-1/C-1 J value = 169 Hz, measured from the residual direct correlation observed in the HMBC spectrum, in agreement with that reported for the alpha anomer of rhamnopyranose (Kasai et al., 1979). Glycosidation shifts were observed for C-1 (δ 84.3), C-26 (δ 72.1), C-3$_{rha}$ (δ 82.6) and C-2$_{ara}$ (δ 75.3). An unambiguous determination of the sequence and linkage sites was obtained from the HMBC spectrum, which showed key correlation peaks between the proton signal at δ 4.30 (H-1$_{ara}$) and the carbon resonance at δ 84.3 (C-1), δ 5.33 (H-1$_{rha}$) and δ 75.3 (C-4$_{ara}$), δ 4.57 (H-1$_{glcI}$) and δ 82.6 (C-3$_{rha}$), and the proton signal at δ 4.31 (H-1$_{glcII}$) and the carbon resonance at δ 72.1 (C-26). On the basis of all these evidences, the structure of the new compound **5** was established as 26-*O*-β-D-glucopyranosyl-furosta-5,20(22),25(27)-triene-1β,3β,26-triol 1-*O*-[β-D-glucopyranosyl-(1→3)-*O*-α-L-rhamnopyranosyl-(1→2)-*O*-α-L-arabinopyranoside].

The analysis of full and tandem mass experiments allowed to assign compound **7** to the same saponin family of **5**, showing as only main differences the presence of the product ion originated by the neutral loss of a 7-hydroxy-6-methylheptan-3-one moiety, ascertaining the lack in **7** of an exomethylene group, a lower number of sugar units, and an aglycon moiety having a molecular weight 2 a.m.u. greater (Table 1). According to this result, the ^{1}H and ^{13}C NMR data of aglycon portion of compound **7** in comparison to those of aglycon portion of **5** clearly suggested that **7** differed from **5** only by the replacement of the exomethylene group with a secondary methyl group at C-27 (δ_H 0.98, δ_C 17.1). Thus, the aglycon of **7** was established as (25*R*)-furosta-5,20(22)-diene-1β,3β,26-triol. The C-25 configuration was deduced to be *R* based on the difference of chemical shifts ($\Delta_{ab} = \delta_a - \delta_b$) of the geminal protons at H$_2$-26 (Δ_{ab} = 0.34 ppm). It has been described that δ_{ab} is usually >0.57 ppm in 25*S* compounds and <0.48 in 25*R* compounds (Agrawal, 2004). The 25*R* configuration was confirmed by hydrolysis of compound **7** with β-glucosidase providing the corresponding spirostanol glycoside. The NMR data of its aglycon moiety were in agreement with those reported for (25*R*)-spirost-5-ene-1β,3β-diol or ruscogenin (Agrawal et al., 1985).

A detailed comparison of NMR data of sugar portion of compound **7** with those of compound **5** showed the absence of the β-glucopyranosyl unit at C-3 of α-rhamnopyranosyl unit. Therefore, compound **7** was identified as the new (25*R*)-26-*O*-β-D-glucopyranosyl-furosta-5,20(22)-diene-1β,3β,26-triol 1-*O*-[α-L-rhamnopyranosyl-(1→2)-*O*-α-L-arabinopyranoside].

In agreement with HPLC–ESIMS^n results, the analysis of ESIMS and ESIMS^n spectra of **8** provided to assign it to a saponin class different from the furostanolic, lacking the typical $[(M-ROH)+H]^+$ ion peak, and from compounds **5** and **7**, which showed product ions originated by neutral loss of 142 or 144 a.m.u. On the contrary,

Table 2
^{13}C and ^{1}H NMR data (J in Hz) of the aglycon moieties of compounds **5**, **7** and **8** (600 MHz, CD_3OD).

	5		**7**[a]		**8**	
	δ_C	δ_H	δ_C	δ_H	δ_C	δ_H
1	84.3	3.40 *dd* (11.9, 3.9)	84.1	3.53 *dd* (11.9, 3.9)	84.3	3.40 *dd* (11.9, 3.9)
2	37.4	2.16, 1.69 *m*	37.3	2.11, 1.71 *m*	37.1	2.13, 1.71 *m*
3	68.8	3.38 *m*	69.0	3.39 *m*	68.8	3.38 *m*
4	43.4	2.28, 2.24 *m*	43.2	2.27, 2.24 *m*	43.2	2.28, 2.24 *m*
5	139.5	–	139.4	–	139.4	–
6	125.7	5.59 *br d* (5.7)	125.7	5.59 *br d* (5.7)	125.3	5.59 *br d* (5.7)
7	32.6	1.99, 1.56 *m*	32.6	1.99, 1.57 *m*	32.4	2.01, 1.58 *m*
8	34.2	1.56 *m*	33.8	1.55 *m*	33.8	1.57 *m*
9	51.2	1.28 *m*	51.2	1.38 *m*	51.2	1.32 *m*
10	43.2	–	43.3	–	43.2	–
11	24.5	2.58, 1.47 *m*	24.6	2.53, 1.47 *m*	24.0	2.64, 1.49 *m*
12	40.7	1.75, 1.34 *m*	41.0	1.73, 1.34 *m*	39.1	1.76, 1.26 *m*
13	43.7	–	44.1	–	41.9	–
14	56.2	1.08 *m*	56.2	1.12 *m*	55.7	1.18 *m*
15	35.6	2.20, 1.44 *m*	34.9	2.18, 1.44 *m*	34.0	2.32, 1.50 *m*
16	85.7	4.74 *dt* (10.1, 7.8, 5.3)	85.2	4.74 *dt* (10.1, 7.8, 5.3)	84.5	5.04 *m*
17	65.9	2.51 *d* (10.1)	65.5	2.51 *d* (10.1)	60.1	1.99 *d* (7.5)
18	14.5	0.75 *s*	14.6	0.75 *s*	14.3	0.80 *s*
19	15.1	1.13 *s*	15.1	1.12 *s*	14.9	1.14 *s*
20	105.4	–	105.5	–	37.5	2.65 *q* (7.5)
21	11.4	1.63 *s*	11.5	1.64 *s*	17.9	1.32 *d* (7.5)
22	152.1	–	152.7	–	184.1	–
23	24.6	2.30 (2H) *m*	24.0	2.16, 1.37 *m*		
24	31.0	2.29 (2H) *m*	31.3	1.65, 1.41 *m*		
25	146.4	–	34.1	1.79 *m*		
26	72.1	4.36 *d* (12.1) 4.15 *d* (12.1)	75.7	3.76, 3.42 *m*		
27	112.7	5.13 *br s* 4.96 *br s*	17.1	0.98 *d* (6.6)		

[a] The chemical shift values of the aglycon moiety of **19** deviate from the experimental values of **7** of ±0.03 ppm.

the ESIMS[2] spectrum highlighted the presence of a product ion at *m/z* 617, due to the neutral loss of 44 a.m.u. due to a CO_2 moiety, together with two product ions, at *m/z* 515 and 383, due to consecutive neutral losses of one deoxy-hexose and one pentose sugar. The IR spectrum of **8** showed an absorption peak at 1745 cm^{-1} due to a carbonyl group. For the aglycon portion in the ^1H NMR spectrum (Table 2) two tertiary methyl groups at δ 1.14 (3H, *s*) and 0.80 (3H, *s*), a secondary methyl group at δ 1.32 (3H, *d*, *J* = 7.5 Hz), an olefinic proton at δ 5.59 (1H, *br d*, *J* = 5.5 Hz), three methine proton signals at δ 5.04 (1H, *m*), 3.40 (1H, *dd*, *J* = 11.9, 3.9 Hz) and 3.38 (1H, *m*), indicative of secondary alcoholic functions, were observed. The NMR data of the aglycon portion of **8** in comparison to those reported for vespertilin (Gonzalez et al., 1971) revealed that the aglycon of **8** differed from vespertilin only by the presence of a secondary alcoholic function to C-1. HBMC correlations between H-16 (δ 5.04), H-17 (δ 1.99), H-20 (δ 2.65), Me-21 (δ 1.32) and the carbonyl group at δ 184.1 along with the downfield shifts of H-16 (δ 5.04) and C-16 (δ 84.5) signals confirmed the presence of a five-membered lactone ring between C-22 and C-16. Additionally, the relative configuration of C-20 was derived by the NOE correlations between H-14α (δ 1.18), H-16 (δ 5.04) and H-17 (δ 1.99) signals, between H-16 (δ 5.04) and H-17 (δ 1.99) signals, between H-17 (δ 1.99) and Me-21 (δ 1.32) signals and between Me-18 (δ 0.80) and H-20 (δ 2.65) signals. On the basis of these data the aglycon of **8** was identified as the new vespertilin derivative (20*S*)-1β,3β,16β-trihydroxypregn-5-ene-20-carboxylic acid 22,16-lactone. Vespertilin, also reported as diosgeninlactone, has been isolated for the first time from the ethanolic extract of the fruits of *Solanum vespertilio* (Gonzalez et al., 1971). Products containing the 22,16-γ-lactone moiety have been isolated from different vegetable sources and postulated to be metabolic products of the corresponding sapogenins. Thus, lactone-type sapogenols and their glycosides might be biosynthetically derived from the genuine 23,26-oxygenated spirostane- or furostane-type (Nafady et al., 2003). Additionally, the ^1H NMR of compound **8** displayed signals for two anomeric proton at δ 5.33 (1H, *d*, *J* = 1.2 Hz) and 4.30 (1H, *d*, *J* = 3.7 Hz) along with a secondary methyl group at δ 1.28 (3H, *d*, *J* = 6.0 Hz). Comparison of NMR data of the sugar portion of compound **8** with those of compound **7** showed that the disaccharide chain at C-1 of the aglycon portion was identical in the two compounds. Thus, compound **8** was identified as the new (20*S*)-1β,3β,16β-trihydroxypregn-5-ene-20-carboxylic acid 22,16-lactone 1-*O*-[α-L-rhamnopyranosyl-(1→4)-*O*-β-D-glucopyranoside].

The analysis of ESIMS and ESIMS^n spectra of **19** showed in the full ESIMS spectrum the $[M+H]^+$ ion peak at *m/z* 943, and in the ESIMS^n spectra the $[(M-162-144)+H]^+$ product ion at *m/z* 637 along with the product ions originated from the latter by consecutive neutral loss of sugar unit (Table 1). Interestingly, the ESIMS^n fragmentation pattern allowed us to identify in **19** the presence of an acetyl moiety, yielding product ions formed by neutral loss of 60 a.m.u (Table 1). According to mass spectrometric results, the ^1H and ^{13}C NMR chemical shifts of the aglycon moieties of **19** and **7** were almost superimposable (see Table 2) confirming the same aglycon portion. Moreover, for **19** the ^1H NMR spectrum displayed signals for three anomeric protons at δ 5.37 (1H, *d*, *J* = 1.2 Hz), 4.38 (1H, *d*, *J* = 7.5 Hz) and 4.28 (1H, *d*, *J* = 7.5 Hz) along with a secondary methyl group at δ 1.28 (3H, *d*, *J* = 6.0 Hz) and a singlet signal at δ 2.08 (3H, *s*) ascribable to the methyl group of an acetyl group. Complete assignments of the ^1H and ^{13}C NMR signals of the sugar portion were accomplished by HSQC, HMBC, DQF-COSY and 1D-TOCSY experiments which led to the identification of one α-rhamnopyranosyl (δ 5.37) unit, one β-glucopyranosyl (δ 4.28) and one 6-*O*-acetyl-β-glucopyranosyl (δ 4.38) unit. The presence of the acetyl group was suggested by the downfield shifts observed for H_2-6_{glcI} (δ 4.35 and 4.31) and C-6_{glcI} (δ 65.0) (Table 5). This evidence was confirmed by the HMBC correlations between the proton signals at δ 4.35 and 4.31 (H_2-6_{glcI}) and δ 2.08 and the carbon resonance at δ 172.3 ($COCH_3$). Once again, the sugar sequence and the linkage sites were deduced from HSQC and HMBC experiments. The glycosidation shifts on C-1 (δ 84.1), C-26 (δ 75.7) and C-2_{glcI} (δ 79.6) indicated the linkage sites. In the HMBC spectrum key correlation peaks between the proton signal at δ 4.38 (H-1_{glcI}) and the carbon resonance at δ 84.1 (C-1), δ 5.37 (H-1_{rha}) and δ 79.6 (C-2_{glcI}), and the proton signal at δ 4.28 (H-1_{glcII}) and the carbon resonance at δ 75.7 (C-26) were observed. Therefore, compound **19** was established as the new (25*R*)-26-*O*-β-D-glucopyranosyl-furosta-5,20(22)-diene-1β,3β,26-triol 1-*O*-[α-L-rhamnopyranosyl-(1→2)-6-*O*-acetyl-β-D-glucopyranoside].

Full positive ESIMS profile of **15** was in agreement with a furostanol structure, showing the diagnostic $[(M-H_2O)+H]^+$ ion as main peak. Analogously to **19**, the analysis of ESIMS^n spectra of **15** allowed to ascertain once again the presence of an acetyl moiety (Table 1). The ^1H NMR spectrum of **15** showed signals for two tertiary methyl groups at δ 1.12 (3H, *s*) and 0.87 (3H, *s*), three secondary methyl groups at δ 1.28 (3H, *d*, *J* = 6.0 Hz), 1.04 (3H, *d*, *J* = 6.6 Hz) and 0.98 (3H, *d*, *J* = 6.6 Hz), an olefinic proton at δ 5.59 (1H, *br d*, *J* = 5.7 Hz), three methine proton signals at δ 4.40 (1H, *m*), 3.53 (1H, *dd*, *J* = 11.9, 3.9 Hz) and 3.39 (1H, *m*), indicative of secondary alcoholic functions, and two methylene proton signals at δ 3.77 and 3.42 (each 1H, *m*), ascribable to a primary alcoholic function, along with three anomeric protons at δ 5.37 (1H, *d*, *J* = 1.2 Hz), 4.38 (1H, *d*, *J* = 7.5 Hz) and 4.28 (1H, *d*, *J* = 7.5 Hz). The comparison of NMR data of compound **15** with those of compound **19** revealed that compound **15** was the 22-hydroxy derivative of compound **19**. Thus, on the basis of the HSQC and HMBC correlations, the aglycon moiety of compound **15** was identified as furosta-5,25(27)-diene-1β,3β,22α,26-tetrol. The configuration of the hydroxy group at C-22 was established to be α from ROESY correlations between H-20 (δ 2.22) and the protons H-23a (δ 1.85) and H-23b (δ 1.65). Therefore, the structure of compound **15** was identify as (25*R*)-26-*O*-β-D-glucopyranosyl-furost-5-ene-1β,3β,22α,26-tetrol 1-*O*-[α-L-rhamnopyranosyl-(1→2)-6-*O*-acetyl-β-D-glucopyran oside].

As well as for compound **15**, ESIMS^n data of **12** provided information about its furostanol nature, showing a characteristic $[(M-H_2O)+H]^+$ ion at *m/z* 901, and the type of sugar units, yielding product ions due to consecutive neutral losses of two hexose and one deoxy-hexose sugar. The NMR data of **12** were superimposable with those of compound **15** except for the absence of the acetyl group at C-6 of the glucopyranosyl unit linked at C-1 of the aglycon (Table 5). Thus, compound **12** was identified as (25*R*)-26-*O*-β-D-glucopyranosyl-furost-5-ene-1β,3β,22α,26-tetrol 1-*O*-[α-L-rhamnopyranosyl-(1→2)-*O*-β-D-glucopyranoside].

The full ESIMS spectra of **16** and **13** clearly identified these compounds as furostanol-type, showing the $[(M-CH_3OH)+H]^+$ ion as the main peak for both. They could be defined as the 22-methyl ether derivatives of **15** and **12**, respectively, each pair showing the same value of *m/z*, but differing for the *m/z* of the relative $[M+Na]^+$ ion, greater of 14 a.m.u. (Table 1). In particular, it could be asserted that **16** and **13** were naturally occurring compounds in *R. ponticus* leaves ruling out they were artefacts derived from compounds **12** and **15** being detectable in the HPLC–ESIMS profile of the ethanol extract performed without methanol in the mobile phase. This result was confirmed by NMR data (^1H, ^{13}C, 1D-TOCSY, DQF-COSY, HSQC, HMBC, ROESY) of compounds **16** and **13**, being apparent that these compounds differed from **15** and **12**, respectively, only by the presence of a methoxy group instead of a hydroxy group at C-22 (Table 3). Therefore, compound **16** was deduced to be (25*R*)-26-*O*-β-D-glucopyranosyl-22α-methoxy-furost-5-ene-1β,3β,26-triol 1-*O*-[α-L-rhamnopyranosyl-(1→2)-6-*O*-acetyl-β-D-glucopyranoside and compound **13** was established as (25*R*)-26-*O*-β-D-glucopyranosyl-22α-methoxy-furost-5-ene-1β,

Table 3
^{13}C and ^{1}H NMR data (J in Hz) of the aglycon moieties of compounds **14**, **15** and **16** (600 MHz, CD_3OD).

	14		**15**[a]		**16**[a]	
	δ_C	δ_H	δ_C	δ_H	δ_C	δ_H
1	84.2	3.53 *dd* (11.9, 3.9)	84.2	3.53 *dd* (11.9, 3.9)	84.1	3.53 *dd* (11.9, 3.9)
2	36.9	2.10, 1.72 *m*	37.2	2.11, 1.71 *m*	37.1	2.10, 1.72 *m*
3	69.0	3.39 *m*	68.9	3.39 *m*	68.8	3.39 *m*
4	43.2	2.28, 2.24 *m*	43.2	2.27, 2.24 *m*	43.2	2.27, 2.24 *m*
5	139.5	–	139.3	–	139.4	–
6	125.7	5.58 *br d* (5.7)	125.8	5.59 *br d* (5.7)	125.7	5.58 *br d* (5.7)
7	32.4	1.99, 1.58 *m*	32.5	2.00, 1.55 *m*	32.4	1.99, 1.57 *m*
8	33.8	1.57 *m*	33.9	1.57 *m*	34.0	1.57 *m*
9	51.2	1.38 *m*	51.0	1.38 *m*	51.0	1.38 *m*
10	43.1	–	43.0	–	43.4	–
11	24.6	2.58, 1.48 *m*	24.9	2.51, 1.46 *m*	24.4	2.52, 1.47 *m*
12	41.0	1.72, 1.25 *m*	41.0	1.69, 1.25 *m*	40.9	1.69, 1.24 *m*
13	40.9	–	40.5	–	40.6	–
14	57.6	1.20 *m*	57.6	1.21 *m*	57.6	1.20 *m*
15	32.5	2.00, 1.32 *m*	32.6	2.00, 1.32 *m*	32.6	1.99, 1.31 *m*
16	82.3	4.40 *m*	82.4	4.40 *m*	82.1	4.39 *m*
17	65.1	1.76 *m*	64.9	1.77 *m*	65.0	1.76 *m*
18	16.8	0.88 *s*	16.6	0.87 *s*	16.9	0.87 *s*
19	14.9	1.12 *s*	14.7	1.12 *s*	15.1	1.12 *s*
20	41.0	2.21 *m*	40.9	2.22 *m*	40.9	2.22 *m*
21	15.8	1.04 *d* (6.6)	15.7	1.04 *d* (6.6)	16.0	1.04 *d* (6.6)
22	113.4	–	113.9	–	113.7	–
23	32.1	1.93, 1.86 *m*	31.3	1.85, 1.65 *m*	31.3	1.86, 1.65 *m*
24	28.2	2.32, 2.23 *m*	28.9	1.61, 1.17 *m*	29.0	1.64, 1.19 *m*
25	146.9	–	34.7	1.77 *m*	34.8	1.77 *m*
26	72.4	4.37 *d* (12.1) 4.16 *d* (12.1)	75.9	3.77, 3.42 *m*	75.7	3.76, 3.41 *m*
27	111.6	5.12 *br s* 4.96 *br s*	16.9	0.98 *d* (6.6)	17.3	0.98 *d* (6.6)
OCH_3			–		47.4	3.17 *s*

[a] The chemical shift values of the aglycon moieties of **12** and **13** deviate from the experimental values of **15** and **16** of ±0.03 ppm, respectively.

3β,26-triol 1-*O*-[α-L-rhamnopyranosyl-(1→2)-*O*-β-D-glucopyranoside. Compounds **16** and **13** are 22-*O*-methyl ethers derivatives of compounds **15** and **12**, respectively.

The analysis of positive full and multistage mass spectra of **14**, ascertaining its furostanol nature, sugar composition, and acetylated form, allowed to identify the aglycon moiety, resulting of 2 a.m.u. smaller than that of **15** (Table 1). This result was indicative of the presence of an exomethylene group, as supported by the occurrence of product ions obtained by neutral loss of the 6-hydroxymethyl-hept-6-en-3-one moiety (142 a.m.u.). Accordingly, a detailed analysis of NMR data of compound **14** in comparison with those of compound **15** confirmed that the two compounds differed only by the presence of a secondary methyl group at C-27 (δ_H 0.98, δ_C 17.1) instead of the exomethylene group (Table 3). Following the same method of analysis shown for compound **7** to determine the C-25 configuration, the structure of compound **14** was established as (25*R*)-26-*O*-β-D-glucopyranosyl-furost-5-ene-1β,3β,22α,26-tetrol 1-*O*-[α-L-rhamnopyranosyl-(1→2)-6-*O*-acetyl-β-D-glucopyranoside].

The full ESIMS spectrum of compound **20** showed as main peak the $[M+H]^+$ ion at *m/z* 871, suggesting a no furostanolic structure. Besides, the finding in $ESIMS^n$ spectra of the product ion originated by neutral loss of 144 a.m.u. from the $[(M-162)+H]^+$ ion, allowed to claim the presence of a methyl group at C-27. The ^1H NMR spectrum of **20** showed for the aglycon portion signals for three tertiary methyl groups at δ 1.64 (3H, *s*), 1.08 (3H, *s*) and 0.75 (3H, *s*), one secondary methyl group at δ 0.97 (1H, *d*, J = 6.6 Hz), an olefinic proton at δ 5.41 (1H, *br d*, J = 5.7 Hz), two methine proton signals at 4.74 (1H, *dt*, J = 10.1, 7.8, 5.3 Hz) and δ 3.60 (1H, *m*) indicative of secondary alcoholic functions, and two methylene proton signals at δ 3.75 and 3.42 (each 1H, *m*), ascribable to a primary alcoholic function. The NMR data of the aglycon moiety of **20** (Table 4) were in good agreement with those reported for (25*R*)-furosta-5,20(22)-diene-3β,26-diol or pseudodiosgenin (Liu and Chen, 2002). The ^1H NMR of the sugar region displayed signals for three anomeric protons at δ 4.45 (1H, *d*, J = 7.5 Hz), 4.33 (1H, *d*, J = 3.7 Hz) and 4.27 (1H, *d*, J = 7.5 Hz). On the basis of 1D-TOCSY, HSQC, HMBC, DQF-COSY correlations these sugar units was identified as α-arabinopyranose (δ 4.33) and β-glucopyranose (δ 4.45 and 4.27). The linkage sites were determined by the HMBC spectrum, which showed key correlation peaks between the proton signal at δ 4.45 ($H\text{-}1_{glcI}$) and the carbon resonance at δ 79.7 (C-3), δ 4.33 ($H\text{-}1_{ara}$) and δ 80.4 ($C\text{-}4_{glcI}$) and the proton signal at δ 4.27 ($H\text{-}1_{glcII}$) and the carbon resonance at δ 75.7 (C-26). On the basis of this evidence the new compound **20** was deduced to be (25*R*)-26-*O*-β-D-glucopyranosyl-furosta-5,20(22)-diene-3β,26-diol 3-*O*-[α-L-arabinopyranosyl-(1→ 4)-*O*-β-D-glucopyranoside].

The analysis of full ESIMS spectrum provided to identify compound **18** as a furostanol glycoside, showing the typical $[(M-H_2O)+H]^+$ ion at *m/z* 871. Further information about the structure and the sugar units could be obtained by the analysis of $ESIMS^n$ data, highlighting the lacking of exomethylene function and the presence of two hexose and one pentose sugar (Table 1). In agreement with these results, the ^1H and ^{13}C NMR data of compound **18** in comparison with those of compound **20** showed that compound **18** was the 22-hydroxy derivative of compound **20** (Table 4). Thus, compound **18** was identified as (25*R*)-26-*O*-β-D-glucopyranosyl-furost-5-ene-3β,22α,26-triol 3-*O*-[α-L-arabinopyranosyl-(1→4)-O-β-D-glucopyranoside].

Finally, the analysis of full and multistage mass spectra acquired for compound **17** allowed to ascertain only one structural difference between this latter and **18**, being the first the $\Delta^{25,27}$-dehydro-derivative of the second. In fact, compound **17** displayed the $[(M-H_2O)+H]^+$ ion and the main product ions of 2 a.m.u

smaller than the corresponding ions in **18**. The NMR data of compound **17** confirmed that this compound differed from **18** only by the replacement of the secondary methyl group at C-27 with an exomethylene group (Table 4). Therefore, the structure of compound **17** was deduced to be 26-*O*-β-D-glucopyranosyl-furosta-5,25(27)-diene-3β,22α,26-triol 3-*O*-[α-L-arabinopyranosyl-(1→4)-*O*-β-D-glucopyranoside].

In conclusion, the so far described analytical methodology allowed us to clarify the saponin composition of the underground parts and leaves of *R. ponticus*. In particular, the adopted HPLC–ESIMS^n method resulted to be able to give a rapid comparative metabolite profiling of these different parts of the plant, promptly highlighting their similarity and their differences. The careful study of HPLC–ESIMS^n data of each chromatographic compound allowed us to obtain an easy and quick screening of the different type of saponins occurring in this *Ruscus* species, underlining a clear prevalence of furostanol glycoside derivatives in *R. ponticus* leaves rather in the underground parts of the plant, showing this latter a wider structure variety. Moreover, from these results, a characteristic chromatographic elution trend for *R. ponticus* saponins could be drawn, first eluting the furostanol glycosides, followed by their dehydrated forms and by vespertilin derivatives, and finally by pregnane and spirostanol glycosides. In particular, the furostanol glycosides isolated from *R. ponticus* are mainly furosta-5,25(27)-diene-1β,3β,22α,26-tetrol, furosta-5,25(27)-diene-3β,22α,26-triol and furosta-5,20(22),25(27)-triene-1β,3β,26-triol derivatives along with the corresponding (25*R*)-25,27-dihydro-derivatives. Interestingly, the occurrence of dehydrated furostanol derivatives, for the first time isolated from a *Ruscus* species, is an unusual finding which makes unique the saponins profile of *R. ponticus*.

3. Experimental

3.1. General

Optical rotations were measured on a JASCO DIP 1000 polarimeter. IR measurements were obtained on a Bruker IFS-48 spectrometer. NMR experiments were performed on a Bruker DRX-600 spectrometer (Bruker BioSpinGmBH, Rheinstetten, Germany) equipped with a Bruker 5 mm TCI CryoProbe at 300 K. All 2D-NMR spectra were acquired in CD_3OD (99.95%, Sigma–Aldrich) and standard pulse sequences and phase cycling were used for DQF-COSY, HSQC, HMBC and ROESY spectra. The NMR data were processed using UXNMR software. Exact masses were measured by a Voyager DE mass spectrometer equipped with a 337 nm laser and delay extraction and operated in positive ion reflector mode. Samples were analyzed by MALDITOF mass spectrometry. A mixture of analyte solution and α-cyano-4-hydroxycinnamic acid (Sigma) was applied to the metallic sample plate and dried. Mass calibration was performed with the ions from adrenocorticotropic hormone (ACTH) fragment 18–39 human at 2465.1989 Da and α-cyano-4-hydroxycinnamic acid at 190.0504 Da as internal standard. Ethanol extract was analyzed by on-line HPLC–ESIMS^n using a ThermoFinnigan Spectra System HPLC coupled with an LCQ Deca ion trap mass spectrometer (ThermoFinnigan, San Jose', CA, USA). HPLC separation was conducted on a C18 reversed-phase (RP) column (5 μm, 2.1 mm × 250 mm; X-Terra MS C18; Waters, Milford, MA) at a flow rate of 0.2 ml/min. A gradient elution was performed by using H_2O (A) and CH_3CN (B) as mobile phases, from 20% B to 70% B in 25 min. The column effluent was analyzed by ESIMS in positive ion mode and the mass spectra were acquired and processed using the software provided by the manufacturer. The capillary voltage was set at 23 V, the spray voltage at 5 kV and the tube lens offset at 50 V. The capillary temperature was 280 °C. Data were acquired in MS^1 and MS^n scanning modes. By using a syringe pump (flow rate 5 μl/min), each pure compound dissolved in H_2O/CH_3CN (1:1) was infused in the ESI source. Positive ESIMS^n analyses were performed using the same conditions as those for HPLC–ESIMS^n analysis.

Semi-preparative HPLC separations were carried out on a Waters 590 system equipped with a Waters R401 refractive index detector, a Waters XTerra Prep MSC18 column (300 × 7.8 mm i.d.) and a Rheodyne injector.

3.2. Plant material

The underground parts and leaves of *R. ponticus* Wor. were collected in June of 2007 in the area of Tbilisi, in Georgia. Samples of *R. ponticus* were identified by Dr. Jemal Aneli, Department of Botany, Institute of Pharmacochemistry, Tbilisi, Georgia. A voucher specimen (No. 368) has been deposited at this Department.

3.3. Extraction and isolation

The air-dried, powdered underground parts of *R. ponticus* (100 g) were extracted with 70% EtOH, three times at 60 °C. The collected alcohol-aqueous extract was concentrated (21 g) and then suspended in water and partitioned with *n*-BuOH. The BuOH extract was dried under vacuum (8 g). Part of extract (3 g) was subjected to Sephadex LH-20 chromatography, eluting with MeOH to yield 11 combined fractions.

Fractions 29–38 and 51–61 were chromatographed by RP-HPLC (Waters XTerra Prep MSC18 column, 300 × 7.8 mm i.d.), at flow rate 2.0 ml/min, using different mixtures of MeOH:H_2O in isocratic conditions.

Fraction 29–38 (297.8 mg) was chromatographed by RP-HPLC using MeOH–H_2O (50:50) as mobile phase to yield compound **5** (1.2 mg, t_R = 32.8 min). From fraction 51–61 (325.1 mg) compounds **1** (1.3 mg, t_R = 28.4 min), **2** (1.2 mg, t_R = 32.0 min), **3** (1.0 mg, t_R = 33.0 min), **4** (1.1 mg, t_R = 33.5 min), **6** (7.8 mg, t_R = 45.8 min), and **7** (3.4 mg, t_R = 46.5 min) were obtained by RP-HPLC using MeOH–H_2O (40:60) as mobile phase.

The remaining 5 g of BuOH extract of the underground parts was subjected to silica gel column chromatography (120 × 3 cm, 100/160 μm, Merck), eluting with isocratic system chloroform:methanol:water (26:14:3), to yield three combined fractions with different polarity: apolar fraction (0.9 g), media polar (2.6 g) and polar fraction (1.3 g).

Apolar fraction was chromatographed by RP-HPLC (flow rate 2.0 ml/min) using MeOH–H_2O (54:46) as mobile phase to yield compounds **8** (1.4 mg, t_R = 32.5 min), and **9** (2.6 mg, t_R = 40.2 min), and using MeOH–H_2O (66:34) as mobile phase to yield compounds **10** (1.2 mg, t_R = 6.2 min) and **11** (1.2 mg, t_R = 7.4 min).

The air-dried, powdered leaves of *R. ponticus* (100 g) were extracted with 70% EtOH, three times at 60 °C. The collected alcohol-aqueous extract was concentrated (16 g) and suspended in water and successively partitioned with chloroform/*n*-BuOH. The BuOH extract was dried under vacuum (10 g).

Part of the extract (3 g) was subjected to Sephadex LH-20 chromatography, eluting with MeOH to yield 16 combined fractions. Fractions 17, 18, and 19–21 were chromatographed by RP-HPLC (Waters XTerra Prep MSC18 column, 300 × 7.8 mm i.d.), at flow rate 2.0 ml/min, using different mixtures of MeOH:H_2O in isocratic conditions.

Fraction 17 (220.5 mg) was chromatographed by RP-HPLC using MeOH–H_2O (40:60) as mobile phase to yield compounds **13** (1.9 mg, t_R = 26.8 min) and **16** (1.6 mg, t_R = 30.0 min). Fraction 18 (239.7 mg) was chromatographed by RP-HPLC using MeOH–H_2O (40:60) as mobile phase to yield compounds **12** (1.4 mg, t_R = 26.0 min), **14** (1.2 mg, t_R = 29.0 min), **15** (1.6 mg, t_R = 29.6 min),

Table 4
^{13}C and ^{1}H NMR data (*J* in Hz) of the aglycon moieties of compounds **17**, **18** and **20** (600 MHz, CD_3OD).

	17		**18**		**20**	
	δ_C	δ_H	δ_C	δ_H	δ_C	δ_H
1	38.4	1.92, 1.12 *m*	38.4	1.91, 1.11 *m*	38.3	1.91, 1.11 *m*
2	30.4	1.96, 1.34 *m*	30.4	1.96, 1.37 *m*	30.5	1.96, 1.33 *m*
3	79.6	3.60 *m*	79.6	3.60 *m*	79.7	3.60 *m*
4	39.4	2.47, 2.30 *m*	39.6	2.46, 2.29 *m*	39.6	2.46, 2.29 *m*
5	141.7	–	141.9	–	142.1	–
6	122.3	5.42 *br d* (5.7)	122.4	5.41 *br d* (5.7)	122.5	5.41 *br d* (5.7)
7	32.6	2.00, 1.60 *m*	32.6	1.99, 1.57 *m*	32.9	2.06, 1.59 *m*
8	32.6	1.71 *m*	32.7	1.70 *m*	32.5	1.70 *m*
9	51.6	1.02 *m*	51.3	1.01 *m*	51.6	1.00 *m*
10	38.0	–	39.0	–	38.0	–
11	21.8	1.59 (2H) *m*	21.8	1.59 (2H) *m*	21.8	1.59 (2H) *m*
12	40.5	1.82, 1.23 *m*	40.5	1.83, 1.24 *m*	40.7	1.82, 1.20 *m*
13	41.5	–	41.7	–	43.4	–
14	57.4	1.18 *m*	57.6	1.18 *m*	56.2	1.12 *m*
15	32.6	2.00, 1.32 *m*	32.7	2.02, 1.32 *m*	34.9	2.18, 1.45 *m*
16	82.1	4.40 *m*	82.3	4.40 *m*	85.2	4.74 *dt* (10.1, 7.8, 5.3)
17	64.9	1.77 *m*	64.9	1.76 *m*	65.5	2.52 *d* (10.1)
18	16.8	0.87 *s*	16.8	0.87 *s*	14.6	0.75 *s*
19	19.6	1.09 *s*	19.8	1.08 *s*	19.6	1.08 *s*
20	41.0	2.22 *m*	41.0	2.21 *m*	105.3	–
21	16.2	1.04 *d* (6.6)	16.0	1.04 *d* (6.6)	11.6	1.64 *s*
22	113.4		114.3	–	152.7	–
23	32.1	1.93, 1.86 *m*	31.3	1.85, 1.65 *m*	23.8	2.15, 1.37 *m*
24	28.2	2.32, 2.23 *m*	28.5	1.62, 1.19 *m*	31.1	1.66, 1.41 *m*
25	147.3	–	34.7	1.77 *m*	34.1	1.79 *m*
26	72.4	4.37 *d* (12.1) 4.15 *d* (12.1)	75.7	3.76, 3.42 *m*	75.7	3.75, 3.42 *m*
27	112.0	5.12 *br s* 4.96 *br s*	17.1	0.98 *d* (6.6)	17.1	0.97 *d* (6.6)

17 (1.3 mg, t_R = 40.2 min), and **18** (1.1 mg, t_R = 40.8 min). From fraction 19–21 (384.1 mg) compounds **19** (1.1 mg, t_R = 30.6 min) and **20** (1.4 mg, t_R = 35.0 min) were obtained by RP-HPLC using MeOH–H_2O (54:46) as mobile phase.

*3.4. 26-O-β-D-glucopyranosyl-furosta-5,20(22),25(27)-triene-1β,3β,26-triol 1-O-[β-D-glucopyranosyl-(1→3)-O-α-L-rhamnopyranosyl-(1→2)-O-α-L-arabinopyranoside] (**5**)*

Amorphous white solid; $C_{50}H_{78}O_{22}$; $[\alpha]_D^{22}$ −25.5° (*c* 0.1 MeOH); IR ν_{max}^{KBr} cm^{-1}: 3429 (>OH), 2920 (>CH), 1260 and 1041 (C–O–C); for ^{1}H and ^{13}C NMR (CD_3OD, 600 MHz) data of the aglycon moiety and the sugar portion see Tables 2 and 5, respectively; HRMALDI-TOFMS $[M+Na]^+$ *m/z* 1053,4890 (calc. for $C_{50}H_{78}O_{22}Na$, 1053,4882).

*3.5. (25R)-26-O-β-D-glucopyranosyl-furosta-5,20(22)-diene-1β,3β,26-triol 1-O-[α-L-rhamnopyranosyl-(1→2)-O-α-L-arabinopyranoside] (**7**)*

Amorphous white solid; $C_{44}H_{70}O_{17}$; $[\alpha]_D^{22}$ −20.3° (*c* 0.1 MeOH); IR ν_{max}^{KBr} cm^{-1}: 3436 (>OH), 2945 (>CH), 1272 and 1048 (C–O–C); for ^{1}H and ^{13}C NMR (CD_3OD, 600 MHz) data of the aglycon moiety and the sugar portion see Tables 2 and 5, respectively; HRMALDI-TOFMS $[M+Na]^+$ *m/z* 893,4519 (calc. for $C_{44}H_{70}O_{17}Na$, 893,4511).

*3.6. (20S)-1β,3β,16β-trihydroxypregn-5-ene-20-carboxylic acid 22,16-lactone 1-O-[α-L-rhamnopyranosyl-(1→4)-O-β-D-glucopyranoside] (**8**)*

Amorphous white solid; $C_{33}H_{50}O_{12}$; $[\alpha]_D^{22}$ −58.4° (*c* 0.1 MeOH); IR ν_{max}^{KBr} cm^{-1}: 3418 (>OH), 2920 (>CH), 1745 (γ-lactone), 1259 and 1064 (C–O–C); for ^{1}H and ^{13}C NMR (CD_3OD, 600 MHz) data of the aglycon moiety and the sugar portion see Tables 2 and 5, respectively; HRMALDITOFMS $[M+Na]^+$ *m/z* 661,3209 (calc. for $C_{33}H_{50}O_{12}Na$, 661,3200).

*3.7. (25R)-26-O-β-D-glucopyranosyl-furost-5-ene-1β,3β,22α,26-tetrol 1-O-[α-L-rhamnopyranosyl-(1→2)-O-β-D-glucopyranoside] (**12**)*

Amorphous white solid; $C_{45}H_{74}O_{19}$; $[\alpha]_D^{22}$ −40.8° (*c* 0.1 MeOH); IR ν_{max}^{KBr} cm^{-1}: 3479 (>OH), 2950 (>CH), 1270 and 1051 (C–O–C); for ^{1}H and ^{13}C NMR (CD_3OD, 600 MHz) data of the aglycon moiety and the sugar portion see Tables 3 and 5, respectively; HRMALDI-TOFMS $[M+Na]^+$ *m/z* 941,4732 (calc. for $C_{45}H_{74}O_{19}Na$, 941,4722).

*3.8. (25R)-26-O-β-D-glucopyranosyl-22α-methoxy-furost-5-ene-1β,3β,26-triol 1-O-[α-L-rhamnopyranosyl-(1→2)-O-β-D-glucopyranoside] (**13**)*

Amorphous white solid; $C_{46}H_{76}O_{19}$; $[\alpha]_D^{22}$ −51.4° (*c* 0.1 MeOH); IR ν_{max}^{KBr} cm^{-1}: 3461 (>OH), 2933 (>CH), 1261 and 1048 (C–O–C); for ^{1}H and ^{13}C NMR (CD_3OD, 600 MHz) data of the aglycon moiety and the sugar portion see Tables 3 and 5, respectively; HRMALDI-TOFMS $[M+Na]^+$ *m/z* 955,4885 (calc. for $C_{46}H_{76}O_{19}Na$, 955,4878).

*3.9. (25R)-26-O-β-D-glucopyranosyl-furost-5-ene-1β,3β,22α,26-tetrol 1-O-[α-L-rhamnopyranosyl-(1→2)-6-O-acetyl-β-D-glucopyranoside] (**14**)*

Amorphous white solid; $C_{47}H_{74}O_{20}$; $[\alpha]_D^{22}$ −42.9° (*c* 0.1 MeOH); IR ν_{max}^{KBr} cm^{-1}: 3478 (>OH), 2938 (>CH), 1740 (C=O), 1265 and 1069 (C–O–C); for ^{1}H and ^{13}C NMR (CD_3OD, 600 MHz) data of the aglycon moiety and the sugar portion see Tables 3 and 5, respectively; HRMALDITOFMS $[M+Na]^+$ *m/z* 981,4679 (calc. for $C_{47}H_{74}O_{20}Na$, 981,4671).

*3.10. (25R)-26-O-β-D-glucopyranosyl-furost-5-ene-1β,3β,22α,26-tetrol 1-O-[α-L-rhamnopyranosyl-(1→2)-6-O-acetyl-β-D-glucopyranoside] (**15**)*

Amorphous white solid; $C_{47}H_{76}O_{20}$; $[\alpha]_D^{22}$ −45.8° (*c* 0.1 MeOH); IR ν_{max}^{KBr} cm^{-1}: 3458 (>OH), 2947 (>CH), 1737 (C=O), 1284 and

1057 (C–O–C); for ^{1}H and ^{13}C NMR (CD_3OD, 600 MHz) data of the aglycon moiety and the sugar portion see Tables 3 and 5, respectively; HRMALDITOFMS $[M+Na]^+$ *m/z* 983,4834 (calc. for $C_{47}H_{76}O_{20}Na$, 983,4828).

3.11. (25R)-26-O-β-D-glucopyranosyl-22α-methoxy-furost-5-ene-1β,3β,26-triol 1-O-[α-L-rhamnopyranosyl-(1→2)-6-O-acetyl-β-D-glucopyranoside] (**16**)

Amorphous white solid; $C_{48}H_{78}O_{20}$; $[\alpha]_D^{22}$ −57.3° (*c* 0.1 MeOH); IR ν_{max}^{KBr} cm^{-1}: 3480 (>OH), 2946 (>CH), 1732 (C=O), 1278 and 1062 (C–O–C); for ^{1}H and ^{13}C NMR (CD_3OD, 600 MHz) data of the aglycon moiety and the sugar portion see Tables 3 and 5, respectively; HRMALDITOFMS $[M+H]^+$ *m/z* 997,4992 (calc. for $C_{48}H_{78}O_{20}Na$, 997,4984).

3.12. 26-O-β-D-glucopyranosyl-furosta-5,25(27)-diene-3β,22α,26-triol 3-O-[α-L-arabinopyranosyl-(1→4)-O-β-D-glucopyranoside] (**17**)

Amorphous white solid; $C_{44}H_{70}O_{18}$; $[\alpha]_D^{22}$ −72.6° (*c* 0.1 MeOH); IR ν_{max}^{KBr} cm^{-1}: 3463 (>OH), 2941 (>CH), 1264 and 1062 (C–O–C); for ^{1}H and ^{13}C NMR (CD_3OD, 600 MHz) data of the aglycon moiety and the sugar portion see Tables 4 and 5, respectively; HRMALDITOFMS $[M+Na]^+$ *m/z* 909,4467 (calc. for $C_{44}H_{70}O_{18}Na$, 909,4460).

3.13. (25R)-26-O-β-D-glucopyranosyl-furost-5-ene-3β,22α,26-triol 3-O-{α-L-arabinopyranosyl-(1→4)-O-β-D-glucopyranoside (**18**)

Amorphous white solid; $C_{44}H_{72}O_{18}$; $[\alpha]_D^{22}$ −67.2° (*c* 0.1 MeOH); IR ν_{max}^{KBr} cm^{-1}: 3451 (>OH), 2930 (>CH), 1275 and 1040 (C–O–C); for ^{1}H and ^{13}C NMR (CD_3OD, 600 MHz) data of the aglycon moiety and the sugar portion see Tables 4 and 5, respectively; HRMALDITOFMS $[M+Na]^+$ *m/z* 911,4625 (calc. for $C_{44}H_{72}O_{18}Na$, 911,4616).

3.14. (25R)-26-O-β-D-glucopyranosyl-furosta-5,20(22)-diene-1β,3β,26-triol 1-O-[α-L-rhamnopyranosyl-(1→2)-6-O-acetyl-β-D-glucopyranoside] (**19**)

Amorphous white solid; $C_{47}H_{74}O_{19}$; $[\alpha]_D^{22}$ −31.0° (*c* 0.1 MeOH); IR ν_{max}^{KBr} cm^{-1}: 3444 (>OH), 2938 (>CH), 1735 (C=O), 1277 and 1054 (C–O–C); for ^{1}H and ^{13}C NMR (CD_3OD, 600 MHz) data of the aglycon moiety and the sugar portion see Tables 2 and 5, respectively; HRMALDITOFMS $[M+Na]^+$ *m/z* 965,4731 (calc. for $C_{45}H_{74}O_{19}Na$, 965,4722).

3.15. (25R)-26-O-β-D-glucopyranosyl-furosta-5,20(22)-diene-3β,26-diol 3-O-[α-L-arabinopyranosyl-(1→4)-O-β-D-glucopyranoside] (**20**)

Amorphous white solid; $C_{44}H_{70}O_{17}$; $[\alpha]_D^{22}$ −55.0° (*c* 0.1 MeOH); IR ν_{max}^{KBr} cm^{-1}: 3468 (>OH), 2953 (>CH), 1280 and 1043 (C–O–C);

Table 5
^{13}C and ^{1}H NMR data (*J* in Hz) of the sugar portions of compounds **5**, **7**, **12**, **18** and **19** (600 MHz, CD_3OD).

	5		**7**[a]		**12**[a]		**18**[b]		**19**[c]	
		α-L-Ara		α-L-Ara		β-D-Glcl		β-D-Glcl		6-*O*-Ac-β-D-Glcl
1	100.9	4.30 *d* (3.7)	100.6	4.30 *d* (3.7)	100.0	4.40 *d* (7.5)	101.8	4.45 *d* (7.5)	100.5	4.38 *d* (7.5)
2	75.3	3.73 *dd* (8.5, 3.7)	75.2	3.73 *dd* (8.5, 3.7)	77.3	3.44 *dd* (9.0, 7.5)	74.6	3.24 *dd* (9.0, 7.5)	77.2	3.44 *dd* (9.0, 7.5)
3	75.9	3.67 *dd* (8.5, 3.0)	75.7	3.67 *dd* (8.5, 3.0)	79.6	3.50 *dd* (9.0, 9.0)	76.0	3.55 *dd* (9.0, 9.0)	79.6	3.51 *dd* (9.0, 9.0)
4	70.6	3.77 *m*	70.5	3.76 *m*	71.8	3.32 *dd* (9.0, 9.0)	80.4	3.57 *dd* (9.0, 9.0)	72.2	3.19 *dd* (9.0, 9.0)
5	67.3	3.88 *dd* (11.9, 2.0) 3.54 *dd* (11.9, 3.0)	67.1	3.87 *dd* (11.9, 2.0) 3.52 *dd* (11.9, 3.0)	77.6	3.27 *ddd* (9.0, 4.5, 2.0)	76.3	3.45 *ddd* (9.0, 4.5, 2.0)	74.2	3.45 *ddd* (9.0, 4.5, 2.0)
6					63.4	3.93 *dd* (12.0, 2.0) 3.63 *dd* (12.0, 4.5)	61.2	3.90 *dd* (12.0, 2.0) 3.86 *dd* (12.0, 4.5)	65.0	4.35 *dd* (12.0, 2.1) 4.31 *dd* (12.0, 4.5)
$OCOCH_3$									172.3	–
$OCOCH_3$									20.8	2.08 *s*
		α-L-Rha		α-L-Rha		α-L-Rha		α-L-Ara		α-L-Rha
1	101.2	5.33 *d* (1.2)	101.2	5.33 *d* (1.2)	101.0	5.37 *d* (1.2)	105.1	4.33 *d* (3.7)	101.1	5.37 *d* (1.2)
2	71.2	4.19 *dd* (3.2, 1.2)	72.1	3.91 *dd* (3.2, 1.2)	72.0	3.91 *dd* (3.2, 1.2)	72.1	3.59 *dd* (8.5, 3.7)	72.1	3.92 *dd* (3.2, 1.2)
3	82.6	3.84 *dd* (9.3, 3.2)	71.8	3.72 *dd* (9.3, 3.2)	71.8	3.71 *dd* (9.3, 3.2)	74.1	3.55 *dd* (8.5, 3.0)	71.9	3.72 *dd* (9.3, 3.2)
4	72.4	3.61 *t* (9.3)	73.8	3.43 *t* (9.3)	73.8	3.42 *t* (9.3)	69.8	3.85 *m*	73.9	3.43 *t* (9.3)
5	69.0	4.18 *m*	69.3	4.11 *m*	69.3	4.12 *m*	67.3	3.96 *dd* (11.9, 2.0) 3.66 *dd* (11.9, 3.0)	69.4	4.13 *m*
6	18.1	1.29 *d* (6.0)	18.2	1.28 *d* (6.0)	18.2	1.27 *d* (6.0)			18.0	1.28 *d* (6.0)
		β-D-Glcl		β-D-Glc		β-D-GlcII		β-D-GlcII		β-D-GlcII
1	105.6	4.57 *d* (7.5)	104.4	4.27 *d* (7.5)	104.3	4.27 *d* (7.5)	104.3	4.27 *d* (7.5)	104.2	4.28 *d* (7.5)
2	75.1	3.33 *dd* (9.0, 7.5)	74.9	3.22 *dd* (9.0, 7.5)	74.8	3.22 *dd* (9.0, 7.5)	74.6	3.23 *dd* (9.0, 7.5)	74.9	3.22 *dd* (9.0, 7.5)
3	77.8	3.40 *dd* (9.0, 9.0)	77.7	3.37 *dd* (9.0, 9.0)	77.7	3.38 *dd* (9.0, 9.0)	77.7	3.38 *dd* (9.0, 9.0)	77.8	3.39 *dd* (9.0, 9.0)
4	71.0	3.38 *dd* (9.0, 9.0)	71.5	3.31 *dd* (9.0, 9.0)	71.3	3.31 *dd* (9.0, 9.0)	71.3	3.31 *dd* (9.0, 9.0)	71.4	3.32 *dd* (9.0, 9.0)
5	77.8	3.28 *ddd* (9.0, 4.5, 2.0)	77.7	3.29 *ddd* (9.0, 4.5, 2.0)	77.6	3.30 *ddd* (9.0, 4.5, 2.0)	77.6	3.29 *ddd* (9.0, 4.5, 2.0)	77.5	3.30 *ddd* (9.0, 4.5, 2.0)
6	62.1	3.88 *dd* (12.0, 2.0) 3.73 *dd* (12.0, 4.5)	62.6	3.90 *dd* (12.0, 2.0) 3.69 *dd* (12.0, 4.5)	62.4	3.89 *dd* (12.0, 2.0) 3.69 *dd* (12.0, 4.5)	62.3	3.89 *dd* (12.0, 2.0) 3.70 *dd* (12.0, 4.5)	62.7	3.90 *dd* (12.0, 2.0) 3.70 *dd* (12.0, 4.5)
		β-D-GlcII								
1	102.9	4.31 *d* (7.5)								
2	74.9	3.24 *dd* (9.0, 7.5)								
3	77.8	3.37 *dd* (9.0, 9.0)								
4	71.3	3.32 *dd* (9.0, 9.0)								
5	77.8	3.28 *ddd* (9.0, 4.5, 2.0)								
6	62.6	3.91 *dd* (12.0, 2.0) 3.69 *dd* (12.0, 4.5)								

[a] The chemical shift values of the sugar portion of **8** and **13** deviate from the experimental values of **7** and **12** respectively, of ±0.03 ppm.
[b] The chemical shift values of the sugar portion of **17** and **20** deviate from the experimental values of **18** of ±0.03 ppm.
[c] The chemical shift values of the sugar portion of **14**–**16** deviate from the experimental values of **19** of ±0.03 ppm.

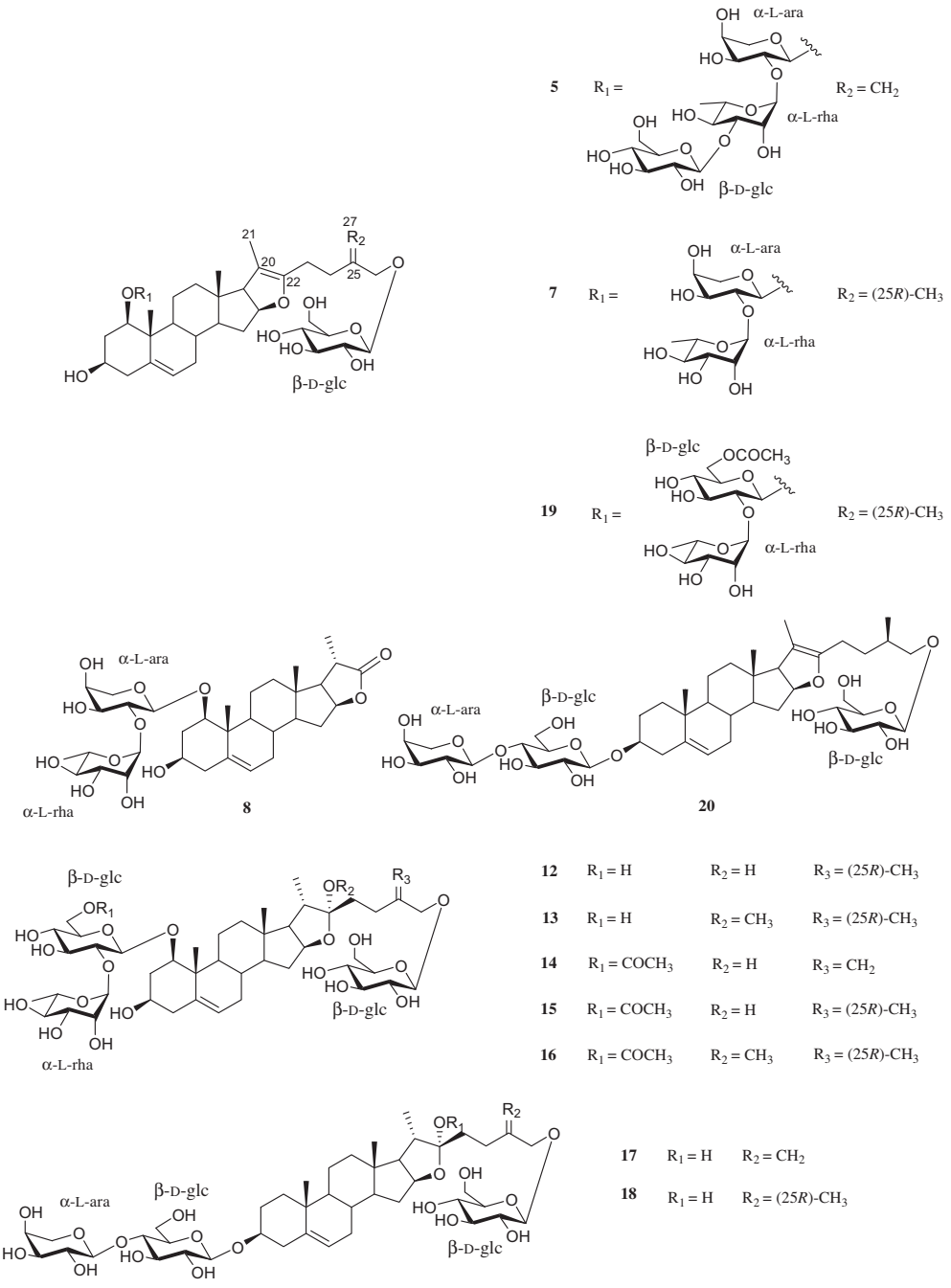

for ^{1}H and ^{13}C NMR (CD_3OD, 600 MHz) data of the aglycon moiety and the sugar portion see Tables 4 and 5, respectively; HRMALDI-TOFMS $[M+Na]^+$ *m/z* 893,4517 (calc. for $C_{44}H_{70}O_{17}Na$, 893,4511).

3.16. Acid hydrolysis

The crude saponin mixture (1 g) was heated at 60 °C with 1:1 0.5 N HCl-dioxane (100 ml) for 2 h, and the mixture was then evaporated in vacuo. The residue was partitioned with CH_2Cl_2–H_2O, and the H_2O layer was neutralized with Amberlite MB-3. The H_2O layer was then concentrated and passed through a silica gel column, using $CHCl_3$–MeOH–H_2O (7:1:1.2, lower layer) as eluting solvent to afford glucose, arabinose and rhamnose.

The D configuration glucose and the L configuration of rhamnose and arabinose were established as by comparison of their optical rotation values with those reported in the literature: D-glucose $[\alpha]_D^{23}$ + 52.5, L-rhamnose $[\alpha]_D^{23}$ − 4.4 (Wang et al., 2008), L-arabinose $[\alpha]_D^{23}$ + 105.0 (Belitz et al., 2009). The optical rotations were determined after dissolving the sugars in H_2O and allowing them to stand for 24 h: D-glucose $[\alpha]_D^{23}$ + 53.4 (*c* 0.1), L-arabinose $[\alpha]_D^{23}$ + 106.2 (*c* 0.1), L-rhamnose $[\alpha]_D^{23}$ − 4.9 (*c* 0.1).

3.17. Enzymatic hydrolysis of compound **7**

Compounds **7** (2.8 mg) was treated with 10 mg of β-glucosidase and 5 ml of 0.5% phosphoric acid at 37 °C for 24 h. After cooling, each solution was extracted three times with *n*-BuOH. The *n*-BuOH layers were concentrated and dried with a N_2 draft affording the corresponding spirostanol glycosides characterized by NMR analysis.

The NMR data of the aglycon moiety of the spirostanol derivative of compound **7** were in agreement with those reported for (25*R*)-spirost-5-ene-1β,3β-diol or ruscogenin (Agrawal et al., 1985).

References

Agrawal, P.K., 2004. NMR spectral investigations, part 51. Dependence of ^{1}H NMR chemical shifts of geminal protons of glycosyloxy methylene (H2–26) on the orientation of the 27-methyl group of furostane-type steroidal saponins. Magn. Reson. Chem. 42, 990–993.

Agrawal, P.K., Jain, D.C., Gupta, R.K., Thakur, R.S., 1985. Carbon-13 NMR spectroscopy of steroidal sapogenins and steroidal saponins. Phytochemistry 24, 2479–2496.

Belitz, H.-D., Grosch, W., Schieberle, P., 2009. Food Chemistry, fourth ed. Springer-Verlag, Heidelberg Berlin.

Bombardelli, E., Bonati, A., Gabetta, B., Mustich, G., 1972. Glycosides from rhizomes of *Ruscus aculeatus*. II. Fitoterapia 43, 3–10.

Gagnidze, R., 2005. Vascular Plants of Georgia. A Nomenclatural Checklist. In: Ketskhoveli, N. (Ed.), Tbilisi, Republic of Georgia, p. 247.

Gonzalez, A.G., Garcia Francisco, C., Freire Barreira, R., Suarez Lopez, E., 1971. New sources of steroidal sapogenins. IX. *Solanum vespertilio*. An. Quim. 67, 433–439.

Kasai, E., Ohikara, M., Asakawa, J., Mizutani, K., Tanaka, O., 1979. ^{13}C NMR study of alpha- and beta-anomeric pairs of D-mannopyranosides and L-rhamnopyranosides. Tetrahedron 35, 1427–1432.

Kereselidze, E.V., Pkheidze, T.A., Kemertelidze, E.P., Khardziani, S.D., Dzhaparidze, T.N., Makharadze, Sh.K., 1975. Fibrinolytic activity of *Ruscus ponticus* and *Ruscus hypophyllum* saponins. Soobsch. AN GSSR 78, 485–488.

Korkashvili, T.Sh., Dzhikiya, O.D., Vugalter, M.M., Pkheidze, T.A., Kemertelidze, E.P., 1985. Steroid glycosides of *Ruscus ponticus*. Soobsch. AN GSSR 120, 561–564.

Liu, H.Y., Chen, C.X., 2002. Two new steroidal saponins from *Tacca plantaginea*. Chin. Chem. Lett. 13, 633–636.

Mimaki, Y., Takaashi, Y., Kuroda, M., Sashida, Y., Nikaido, T., 1996. Steroidal saponins from *Nolina recurvata* stems and their inhibitory activity on cyclic AMP phosphodiesterase. Phytochemistry 42, 1609–1615.

Mimaki, Y., Kuroda, M., Kameyama, A., Yokosuka, A., Sashida, Y., 1998. New steroidal constituents of the underground parts of *Ruscus aculeatus* and their cytostatic activity on HL-60 cells. Chem. Pharm. Bull. 46, 298–303.

Mulkijanyan, A.K., Abuladze, G., 1998. Antiinflamatory activity of the steroidal saponins of *Ruscus ponticus*. Proc. Georg. Acad. Sci. 24 (1–6), 265–269.

Mulkijanyan, K., Abuladze, G., 2000. Antiexudative action of steroid glycosides' preparation ruscoponin from *Ruscus ponticus*. Bull. Georg. Acad. Sci. 161, 254–256.

Nafady, A.M., El-Shanawany, M.A., Mohamed, M.H., Hassanean, H.A.-H., Zhu, X.-H., Yoshihara, T., Okawa, M., Ikeda, T., Nohara, T., 2003. Peculiar side-chain fission of steroidal glycosides. Tetrahedron Lett. 44, 3509–3511.

Perrone, A., Muzashvili, T., Napolitano, A., Skhirtladze, A., Kemertelidze, E., Pizza, C., Piacente, S., 2009. Steroidal glycosides from the leaves of *Ruscus colchicus*: isolation and structural elucidation based on a preliminary liquid chromatography–electrospray ionization tandem mass spectrometry profiling. Phytochemistry 70, 2078–2088.

Pkheidze, T.A., Kereselidze, E.V., Kachukhashvili, T.N., Kemertelidze, E.P., 1970. Steroid sapogenins of some Georgian plants. Tr. 1-go Vses. S'ezda Farm. 1967, 215–221.

Pkheidze, T.A., Kereselidze, E.V., Kemertelidze, E.P., 1971. Diosgenin, neoruscogenin, and ruscogenin from *Ruscus ponticus*, *Ruscus hypophyllum*, and *Allium albidum*. Khim. Prir. Soedin. 7, 841–842.

Wang, X.W., Mao, Y., Wang, N.-L., Yao, X.S., 2008. A new phloroglucinol diglycoside derivative from *Hypericum japonicum* Thunb.. Molecules 13, 2796–2803.

Yuan, L., Ji, T.F., Wang, A.G., Yang, J.B., Su, Y.L., 2008. Two new furostanol saponins from the seeds of *Allium cepa* L.. Chin. Chem. Lett. 19, 461–464.